Kinetics and Mechanisms of Molybdate Adsorption/Desorption at the Goethite/Water Interface Using Pressure-Jump Relaxation

Peng Chu Zhang* and Donald L. Sparks

ABSTRACT

Pressure-jump (p-jump) relaxation with conductivity detection was used to ascertain the kinetics and mechanisms of MoO_4 adsorption/desorption on goethite. A postulated reaction mechanism consisting of two consecutive elementary steps was examined and verified through kinetic and equilibrium studies. The first step is the formation of an ion-pair complex through the electrostatic attraction between the protonated surface and the MoO_4 anion. The second step involves a ligand exchange process, whereby 1 mol of H_2O is replaced by 1 mol of adsorbed MoO_4 from the surface. It is much slower than the first step. The forward and backward intrinsic rate constants for steps 1 and 2 are: $k_1^{int} = 4019.2$ mol^{-1} L s^{-1}, $k_{-1}^{int} = 391.5$ s^{-1}, $k_2^{int} = 1.888$ mol^{-1} L s^{-1}, and $k_{-2}^{int} = 42.34$ s^{-1}. A slightly modified triple layer model (TLM) was employed to calculate the distribution of ionic species on the goethite surface, in the α and β layers, and in the bulk solution at equilibrium and electrical parameters for the charged surface. Both equilibrium and kinetic data fit the postulated mechanism for the reaction steps and the modified adsorption model well.

INVESTIGATIONS ON THE KINETICS of adsorption/desorption processes frequently provide important and enlightening information about the state of bonding in the adsorption phase (Wedler, 1976). To properly understand the dynamic interactions between fertilizers, pesticides, organic pollutants and sludges with soils, and to predict the mineral equilibria and geochemical behavior of elements in soils, one must have kinetics information. Additionally, to fully model organic and inorganic reactions in soil, a knowledge of their rates and mechanisms is fundamental (Rai and Muraka, 1987; Sparks, 1987, 1989). An assessment of the kinetic aspects of inorganic ion-soil interactions must precede the application of a thermodynamic-based model (Sposito, 1985).

Many reactions involving adsorption/desorption phenomena on soils and soil constituents are exceeding rapid, often occurring on millisecond and microsecond time scales (Sparks, 1989). Accordingly, batch and flow techniques (see e.g. Sparks, 1989) that are commonly used by most experimentalists are unsatisfactory for measuring such rapid reactions. Another inherent disadvantage of most, if not all, batch and flow techniques is that apparent rate laws and rate parameters are measured since a combination of chemical reaction and mass transfer phenomena are being determined. Consequently, few reports have appeared on the chemical kinetics of inorganic reactions on soil constituent surfaces.

One way to measure the chemical kinetics of rapid reactions on soil constituents is to use relaxation methods. These techniques, including pressure jump (p-jump), stopped flow, and electric field pulse, have been employed in the past 10 yr to study interactions between soil constituents and ionic species (Hachiya et al., 1979; Hachiya et al., 1980; Ikeda et al., 1982; Negishi et al., 1984; Hayes and Leckie, 1986). Unfortunately, soil scientists have not used these techniques in kinetic studies.

Relaxation methods are based on the principle of chemical relaxation which is used to describe the self-adjustment of a perturbed molecular system to its thermal equilibrium. The time ("relaxation time") required in the self-adjustment is related to the specific rates of the chemical reactions involved (Bernasconi, 1976). With relaxation methods, one can measure the reaction rate in millisecond or microsecond time scales and determine the elementary reactions involved. In this paper, a p-jump technique is used to obtain kinetic information on molybdate interactions at the goethite/water interface.

In order to establish the overall equilibrium behavior and reaction stoichiometry of this system, the triple layer model (TLM) was employed. It has several advantages over other equilibrium-based models: analogues for either surface coordination or an ion-pair complex can be chosen, and the background electrolyte surface reactions can be modeled which allows one to test for effects of changing ionic strength on ion adsorption (Hayes and Leckie, 1986). Simulations produced from the model were examined both thermodynamically and kinetically.

Based on the thermodynamic and kinetic information obtained, a mechanism for molybdate adsorption on goethite will be postulated. The mechanism we discuss is concerned with both the physical meaning of molybdate adsorption including where the ad-

Dep. of Plant Science, Univ. of Delaware, Newark, DE 19717-1303. Contribution from the Delaware Agric. Exp. Stn. no. 1064 and the Dep. of Plant Science no. 243. Rec. 17 Oct. 1988. *Corresponding author.

Published in Soil Sci. Soc. Am. J. 53:1028-1034 (1989).

sorbed ions are located, and how the reaction is carried out and what elementary reaction(s) are involved.

MATERIALS AND METHODS

Sample Preparation

The goethite that was used in this study was synthesized according to the procedure described by Atkinson et al. (1967). After freeze-drying, it was examined by x-ray diffraction and the characteristic 0.418-nm peak for goethite was observed. The goethite was then placed in a dialysis tube and dialyzed in deionized water. The water was changed daily until the conductivity of the goethite suspension equaled that of the deionized water. The dialyzed goethite was then dispersed using an ultrasonic disperser. The particle size of the dispersed goethite was <2 μm.

Specific surface area of the goethite which was determined using the ethylene glycol monoethyl ether (EGME) method of Carter et al. (1986), was 70.1×10^3 m^2 kg^{-1}. A potentiometric titration technique was employed to determine the surface site density of the goethite which was 6.4 site nm^{-2} and the intrinsic constants for protonation (K_{a1}^{int}) and deprotonation (K_{a2}^{int}) and the intrinsic constants for background electrolyte reactions on the surfaces ($K_{NO_3}^{int}$ and K_{Na}^{int}) which are defined in Eq. [1] to [4] were determined using the nonlinear least squares optimization program FITEQL (Westall, 1982). The constants used in this investigation are given in Table 1.

Sodium nitrate and HNO_3 were used to adjust the ionic strength and pH, respectively, of the oxide suspension. Sodium molybdate was the adsorptive. All the chemicals that were used were analytical reagents and no further purification was made.

Static Studies

The adsorption studies were carried out by placing a goethite suspension containing a 4.5×10^{-3} mol L^{-1} Na_2MoO_4 solution, and $NaNO_3$ as the background electrolyte, such that the concentration of $NaNO_3$ in the suspension was 0.01, 0.05, or 0.1 mol L^{-1}, into polypropylene centrifuge tubes. The final particle concentration was 15.8 g L^{-1}. The tubes were shaken end-to-end on a reciprocating shaker overnight, centrifuged using a super-speed centrifuge (Sorvall RC-5B, Du Pont Instrument) at $34550 \times g$ for 30 min., and the supernatant solution was then filtered through 0.2-μm matric membrane filter paper. Molybdate and Na concentrations were determined using a Perkin-Elmer 5000 atomic absorption spectrophotometer, NO_3 was measured using ion chromatography, and the pH of the supernatant was determined.

Kinetic Studies

In the kinetic studies, relaxation times (τ values) were measured for the molybdate-oxide suspension at a 0.01 M ionic strength using a Dia-Log p-jump apparatus (DIA-RPC, produced by Dia-log Co., distributed by Inrad Interactive Radiation Inc., Northvale, NJ) and conductivity detector (DIA-RPM, Dia-log Co.). Before analyzing a given MoO_4-goethite suspension kinetically, part of the suspension was separated and analyzed for pH and NO_3, Na, and MoO_4 concentrations using the procedures given previously. During the p-jump relaxation measurement, 9.595 MPa of pressure was established on a cell containing the goethite and molybdate suspension; then the pressure was released within 70 μs by bursting a brass membrane of 0.03-mm thickness. A digitizer (DIA-RRC, Dia-log Co.) was then triggered and the changes in conductivity of the suspension were caught. The signals were digitized and then sent to a microcomputer (AIM 65, Rockwell International Co., Anaheim, CA). The results of the relaxation could be read from the computer print out and displayed on an oscilloscope. The p-jump relaxation and electrical conductivity detection devices are described in detail in Appendix 1.

Application of Modified Triple Layer Model

A modified triple layer adsorption model (TLM), which was used by Hayes and Leckie (1986) to study Pb adsorption on goethite, was employed in this study. The modified TLM differs from the original model (Davis and Leckie, 1980) in two ways: (i) the adsorbed ion can be located at both the α layer and β layer rather than only at the β layer, i.e., the adsorbed ion can form an inner- and/or outer-sphere surface complex, not just an outer-sphere complex; and (ii) the chemical potential and standard and reference states are defined equivalently for both solution and surface species, leading to a different relationship between the activity coefficients and the interfacial potential than previously used. Further details about the TLM and modifications to it can be found in Hayes and Leckie (1986, 1987).

The following chemical reactions can be defined for the application of the TLM to molybdate adsorption on goethite,

$$SOH_2^+ \rightleftharpoons SOH + H^+ \quad [1]$$

$$SOH \rightleftharpoons SO^- + H^+ \quad [2]$$

$$SOH_2^+ + NO_3^- \rightleftharpoons SOH_2^+ - NO_3^- \quad [3]$$

$$SO^- + Na^+ \rightleftharpoons SO^- - Na^+ \quad [4]$$

$$SOH_2^+ + MoO_4^{2-} \rightleftharpoons SOH_2^+ - MoO_4^{2-} \quad [5]$$

$$SOH_2^+ + HMoO_4^- \rightleftharpoons SOH_2^+ - HMoO_4^- \quad [6]$$

where SOH represents 1 mol of reactive surface hydroxyls bound to a Fe ion in goethite. Equations [5] and [6] represent the formation of an outer-sphere surface complex in which molybdate ions are located at the β layer. The intrinsic conditional equilibrium constants are defined using Eq. [7] to [12]:

$$K_{a1}^{int} = \frac{[SOH][H^+]}{[SOH_2^+]} \exp(-F\psi_\alpha/RT) \quad [7]$$

$$K_{a2}^{int} = \frac{[SO^-][H^+]}{[SOH]} \exp(-F\psi_\alpha/RT) \quad [8]$$

$$K_{NO_3^-}^{int} = \frac{[SOH_2^+ - NO_3^-]}{[SOH_2^+][NO_3^-]} \exp[F(\psi_\alpha - \psi_\beta)/RT] \quad [9]$$

$$K_{Na^+}^{int} = \frac{[SO^- - Na^+]}{[SO^-][Na^+]} \exp[-F(\psi_\alpha - \psi_\beta)/RT] \quad [10]$$

$$K_{MoO_4^{2-}}^{int} = \frac{[SOH_2^+ - MoO_4^{2-}]}{[SOH_2^+][MoO_4^{2-}]} \exp[F(\psi_\alpha - 2\psi_\beta)/RT] \quad [11]$$

$$K_{HMoO_4^-}^{int} = \frac{[SOH_2^+ - HMoO_4^-]}{[SOH_2^+][HMoO_4^-]} \exp[F(\psi_\alpha - \psi_\beta)/RT] \quad [12]$$

where F is the Faraday constant, R is the universal gas constant, and T is the absolute temperature. Square brackets indicate concentration and the exponential terms represent the activity coefficients for a charged surface where ψ_α and ψ_β are the electrical potentials at the α and β layer, respectively.

The surface charge balance equations based on the above reactions are

$$\sigma_\alpha = [SOH_2^+] + [SOH_2^+ - NO_3^-] + [SOH_2^+ - HMoO_4^-] + [SOH_2^+ - MoO_4^{2-}] - [SO^-] - [SO^- - Na^+] \quad [13]$$

$$\sigma_\beta = [SO^- - Na^+] - [SOH_2^+ - HMoO_4^-] - 2[SOH_2^+ - MoO_4^{2-}] - [SOH_2^+ - NO_3^-] \quad [14]$$

From the electroneutrality condition,

$$\sigma_\alpha + \sigma_\beta + \sigma_d = 0 \quad [15]$$

where σ_d is the charge at the diffusion layer; it can be calculated using Gouy-Chapman theory and the relationship,

$$\sigma_d = -11.74 C_s^{1/2} \sinh(F\psi_d/2RT) \quad [16]$$

where C_s is the concentration of a symmetrical monovalent electrolyte. The relation between charge and potential are derived assuming that the planes can be treated as plates of two parallel plate capacitors with

$$\sigma_\alpha = C_1(\psi_\alpha - \psi_\beta) \quad \text{and,} \quad [17]$$

$$-\sigma_d = C_2(\psi_\beta - \psi_d) \quad [18]$$

where C_1 and C_2 are the capacitance constants for the α and β plane layers, respectively, which cannot be measured experimentally. The values of C_1 and C_2 in this study are 1.2 and 0.2 F m^{-2}, respectively, and they were determined based on the goodness of fit to the TLM.

In the modified TLM, the molybdate ions are allowed to form an inner-sphere surface coordination complex by placement of the molybdate ions in the α layer such that,

$$SOH_2^+ + MoO_4^{2-} \rightleftharpoons SMoO_4^- + H_2O \quad [19]$$

$$SOH_2^+ + HMoO_4^- \rightleftharpoons SHMoO_4 + H_2O \quad [20]$$

The charge balance for the reactions is then,

$$\sigma_\alpha = [SOH_2^+] + [SOH_2^+ - NO_3^-] - [SMoO_4^-] - [SO^-] - [SO^- - Na^+] \quad [21]$$

$$\sigma_\beta = [SO^- - Na^+] - [SOH_2^+ - NO_3^-] \quad [22]$$

The intrinsic conditional constants for adsorption of molybdate ions in this case would be

$$K^{int}_{MoO_4^{2-}} = \frac{[SMoO_4^-]}{[SOH_2^+][MoO_4^{2-}]} \exp(-F\psi_\alpha/RT) \quad [23]$$

$$K^{int}_{HMoO_4^-} = \frac{[SHMoO_4]}{[SOH_2^+][HMoO_4^-]} \exp(-F\psi_\alpha/RT) \quad [24]$$

In the present study, parameters from both the computed results when the adsorbed molybdate ions are treated as an ion-pair (outer-sphere) surface complex or as a surface coordination (inner-sphere) complex were used to model the reactions thermodynamically and kinetically. It should be mentioned that other equilibrium-based models were tested in this study, however, only the modified TLM fit the observed experimental data well.

RESULTS AND DISCUSSIONS

Static Studies

Results of molybdate (4.5×10^{-3} mol L^{-1}) adsorption on goethite (15.8 g L^{-1}) as a function of pH in three different $NaNO_3$ background electrolyte concentrations (0.01, 0.05, and 0.1 mol L^{-1}) are shown in Fig. 1. There was a small effect of background electrolyte concentration on adsorption at a given pH. The modified TLM was used to model molybdate adsorption for both inner- (Fig. 1) and outer-sphere surface (Fig. 2) complexation at the three ionic strengths. For the inner-sphere case, the simulations agree quite well with the experimental data (Fig. 1). On the other hand, the observed data are not described well assuming that outer-sphere complexation is operational (Fig. 2). In both cases, the constants listed in Table 1 were used in the computations.

Hingston et al. (1972) reported that molybdate adsorption on goethite involves a ligand exchange process which they referred to as specific adsorption. The NO_3 anion, which was present in the background electrolyte solution ($NaNO_3$) that we used, is adsorbed very weakly on colloidal surfaces through electrostatic attractive forces (Parfitt, 1978; Mott, 1981). This type of adsorption is termed nonspecific adsorption. The TLM applied in this paper places ions adsorbed by

Table 1. Intrinsic equilibrium constants for the oxide suspension as determined from the modified TLM.

$\log K^{int}_{a1}$ =	−5.80
$\log K^{int}_{a2}$ =	−11.1
$\log K^{int}_{Na}$ =	−8.80
$\log K^{int}_{NO_3}$ =	7.6

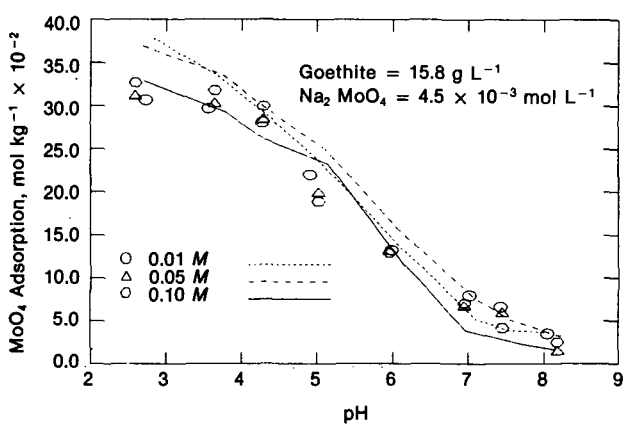

Fig. 1. Adsorption of MoO_4 on goethite vs. pH at three $NaNO_3$ background electrolyte concentrations. Experimental data are applied to the modified TLM assuming inner-sphere surface complexation; symbols represent experimental data and lines represent TLM prediction.

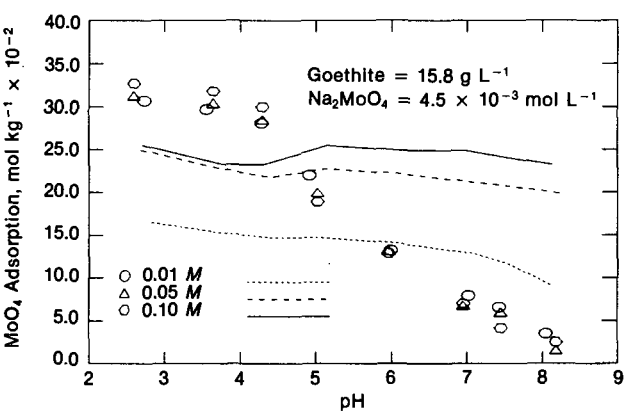

Fig. 2. Adsorption of MoO_4 on goethite vs. pH at three $NaNO_3$ background electrolyte concentrations. Experimental data are applied to the modified TLM assuming outer-sphere surface complexation; symbols represent experimental data and lines represent TLM prediction.

electrostatic forces at the β layer, thus, little or no competition occurs between the molybdate and NO_3 anions.

A previous assumption was that only one molybdate ion reacts with one protonated surface site. The goodness-of-fit of our data to the modified TLM indicates that only 1 mol of ligand was replaced by 1 mol of adsorbed molybdate. Based on this, the stoichiometry of the overall molybdate adsorption on goethite can be established. Furthermore, while modeling molybdate adsorption, the speciation of molybdate ions was considered. In the pH range of 4 to 7 that was employed in this study, the molybdate ion can exist as two species, $HMoO_4^-$ and MoO_4^{2-}, with an association constant (K_2) of 10^{-4}. However, the dominant form of the molybdate anion is MoO_4^{2-} when the pH of the suspension is >4. Based on the modeling of the data, it was found that the major fraction of the goethite-molybdate suspension is $SMoO_4^-$, with the $SHMoO_4$ species existing in a very trace amount (about 10^{-23}–10^{-26} mol L^{-1}). Thus, this latter species can be ignored in our study.

Additionally, by using the modified TLM, we checked the form of the functional group that was directly reacting with molybdate. It was found that the molybdate anions reacted primarily with the protonated site, the SOH_2^+ and not with the neutral one, SOH. For the reactions carried out over a pH range of 4 to 7, the goethite surface is positively charged since the point of zero charge of the goethite is about 8.4. We tried to use neutral sites in our calculation, but the results obtained were not reasonable.

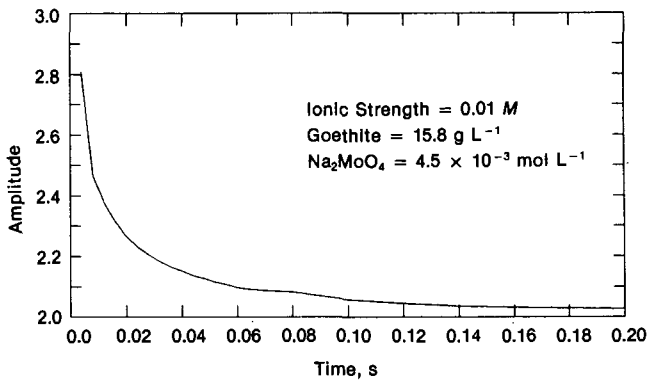

Fig. 3. Typical pressure-jump relaxation curve showing change in conductivity vs. time for the goethite suspension.

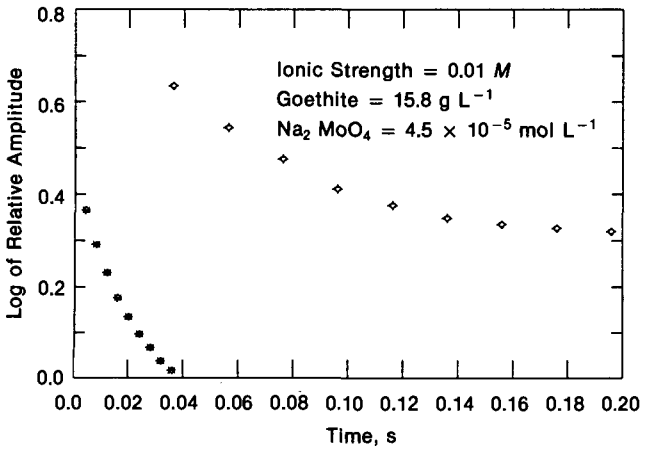

Fig. 4. Semi-log relaxation curves for the goethite suspension.

Kinetic Studies

Kinetics of MoO_4 adsorption on goethite using the p-jump technique with electrical conductivity detection revealed a double relaxation (Fig. 3). The directions of both of the relaxation signals indicate a decrease in conductivity of the suspension during the relaxation. Relaxations were not obtained when a goethite-$NaNO_3$ suspension, the supernatant solution of a goethite-molybdate suspension and only a goethite suspension were examined using p-jump relaxation. However, the concentration of molybdate in suspension significantly decreased after it was equilibrated with goethite. These findings indicate that the relaxations were caused by adsorption/desorption of molybdate at the goethite/water interface.

Determination of reciprocal relaxation time constants (τ_1^{-1} and τ_2^{-1}) were made from semi-log plots of the relaxation curves as shown in Fig. 4. A fast reciprocal relaxation time, τ_1^{-1}, can be separated from a slow one, τ_2^{-1}, based on the significantly different rates of conductivity change as a function of time. Both τ_1^{-1} and τ_2^{-1} increased with increases in pH of the goethite suspensions (Fig. 5). The double relaxation curve that was observed (Fig. 3) following pressure perturbation would indicate that two reactions are operational. Combining the information from the p-jump relaxation studies and from the overall equilibrium partitioning and the reaction stoichiometry, a two-step reaction is postulated to describe the mechanism of molybdate adsorption on goethite

$$SOH_2^+ + MoO_4^{2-} \underset{\text{step 1}}{\rightleftharpoons} SOH_2^+ - MoO_4^{2-} \underset{\text{step 2}}{\rightleftharpoons} SMoO_4^- + H_2O. \quad [25]$$

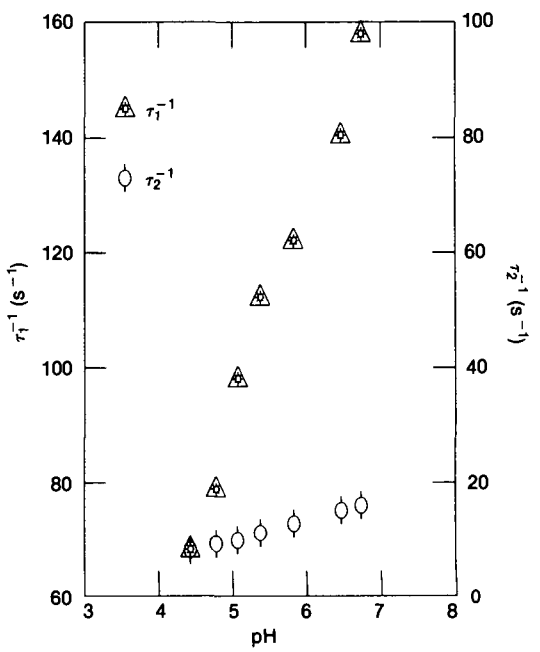

Fig. 5. Relationship between pH and fast (τ_1^{-1}) and slow (τ_2^{-1}) reciprocal relaxation times for the two step reaction given in Eq. [25]).

In the first step, MoO_4 is attracted to the β layer by electrostatic interaction, and forms an ion-pair complex with a protonated surface site. Then, through the second step, MoO_4 replaces a ligand from the surface site to form an inner-sphere surface complex at the α layer. The MoO_4 now occupies the position of the replaced ligand, in this case, the H_2O molecule. The second step in Eq. [25] includes processes of bond breaking and bond formation. The intrinsic conditional equilibrium constants K_1^{int} and K_2^{int} for step 1 and step 2, respectively, are defined as,

$$K_1^{int} = \frac{[SOH_2^+ - MoO_4^{2-}]}{[SOH_2^+][MoO_4^{2-}]} \exp\left[\frac{F(\psi_\alpha - 2\psi_\beta)}{RT}\right] \quad [26]$$

$$K_1^{int} = \frac{k_1^{int}}{k_{-1}^{int}} = K_1 \exp\left[\frac{F(\psi_\alpha - 2\psi_\beta)}{RT}\right] \quad [27]$$

$$K_2^{int} = \frac{[SMoO_4^-]}{[SOH_2^+ - MoO_4^{2-}]} \exp\left(\frac{-F\psi_\alpha}{RT}\right) \quad [28]$$

$$K_2^{int} = \frac{k_2^{int}}{k_{-2}^{int}} = K_2 \exp\left(\frac{-F\psi_\alpha}{RT}\right) \quad [29]$$

where the k_1^{int}, k_{-1}^{int}, k_2^{int} and k_{-2}^{int} are the intrinsic forward (k_1^{int} and k_2^{int}) and backward (k_{-1}^{int} and k_{-2}^{int}) rate constants for step 1 and 2 in Eq. [25]. The electrical potential term used to describe step 1 is associated with the β layer, and that used to describe step 2 is associated with the α layer. The reason for this is that the two steps create different effects at the two layers.

Using the kinetic model described in Eq. [25] and the stoichiometry of the overall reactions, i.e., one molybdate ion replaces one ligand from the protonated surface, the following relationships between τ_1^{-1}, τ_2^{-1} and the reactant concentrations can be derived (see Appendix 2 for more detail)

$$\tau_1^{-1} = k_1^{int}\{\exp\left[\frac{-F(\psi_\alpha - 2\psi_\beta)}{2RT}\right]([SOH_2^+] + [MoO_4^{2-}])\} + k_{-1}^{int}\exp\left[\frac{F(\psi_\alpha - 2\psi_\beta)}{2RT}\right] \quad [30]$$

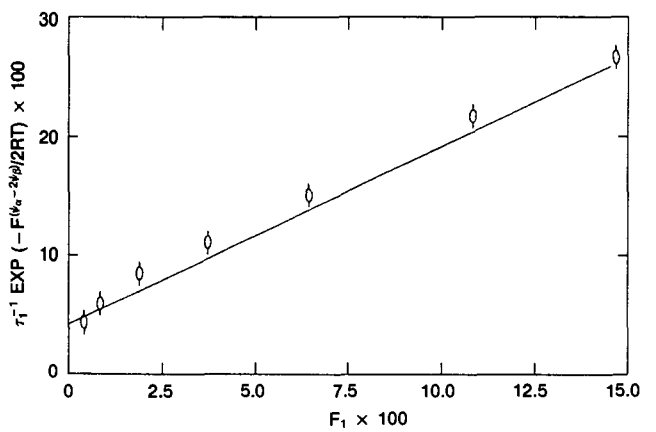

Fig. 6. Plot of $\tau_1^{-1}\exp\left(\frac{-F(\psi_\alpha - 2\psi_\beta)}{2RT}\right)$ vs. F_1 in Eq. [32] to test the mechanism for step 1 as proposed in Eq. [25].

$$\tau_2^{-1} = k_2^{int}\left[\exp\left(\frac{F\psi_\alpha}{2RT}\right)\left\{k_1^{int}\exp\left[\frac{-F(\psi_\alpha - 2\psi_\beta)}{2RT}\right]([SOH_2^+] + [MoO_4^{2-}])\right\} \Big/ \left\{k_1^{int}\exp\left[-\frac{F(\psi_\alpha - 2\psi_\beta)}{2RT}\right]([SOH_2^+] + [MoO_4^{2-}]) + k_{-1}^{int}\exp\left(\frac{F(\psi_\alpha - 2\psi_\beta)}{2RT}\right)\right\}\right] + k_{-2}^{int}\exp\left(\frac{-F\psi_\alpha}{2RT}\right) \quad [31]$$

Rearranging Eq. [30] and [31],

$$\tau_1^{-1}\exp\left[\frac{-F(\psi_\alpha - 2\psi_\beta)}{2RT}\right] = k_1^{int}\{\exp\left[\frac{-F(\psi_\alpha - 2\psi_\beta)}{RT}\right]([SOH_2^+] + [MoO_4^{2-}])\} + k_{-1}^{int} = k_1^{int}F_1 + k_{-1}^{int} \quad [32]$$

$$\tau_2^{-1}\exp\left(\frac{F\psi_\alpha}{2RT}\right) = k_2^{int}\left[\exp\left(\frac{F\psi_\alpha}{RT}\right)\left\{k_1^{int}\exp\left[\frac{-F(\psi_\alpha - 2\psi_\beta)}{2RT}\right]([SOH_2^+] + [MoO_4^{2-}])\right\} \Big/ \left\{k_1^{int}\exp\left[-\frac{F(\psi_\alpha - 2\psi_\beta)}{2RT}\right]([SOH_2^+] + [MoO_4^{2-}]) + k_{-1}^{int}\exp\left(\frac{F(\psi_\alpha - 2\psi_\beta)}{2RT}\right)\right\}\right] + k_{-2}^{int} = k_2^{int}F_2 + k_{-2}^{int} \quad [33]$$

Table 2. Intrinsic rate and equilibrium constants determined from kinetic measurements.

k_1^{int}	k_{-1}^{int}	k_2^{int}	k_{-2}^{int}	K_1^{int}	K_2^{int}
mol^{-1} Ls^{-1}	s^{-1}	mol^{-1} Ls^{-1}	s^{-1}	mol^{-1} L	mol^{-1} L
4019.2	391.5	1.89	42.34	10.28	0.045

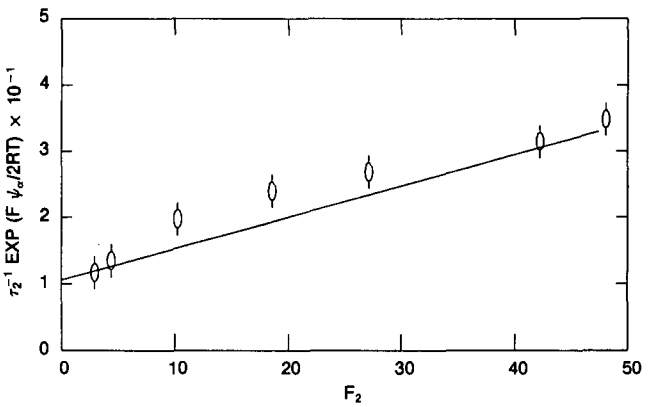

Fig. 7. Plot of $\tau_2^{-1}\exp\left(\frac{F\psi_\alpha}{2RT}\right)$ vs. F_2 in Eq. [33] to test the mechanism for step 2 as proposed in Eq. [25].

If the mechanism proposed in Eq. [25] is consistent with the experimental relaxation data, then plots of τ_1^{-1} and τ_2^{-1} with the exponential terms on the left hand side of Eq. [32] and [33] vs. the concentration terms (F_1 and F_2) on the right hand sides of Eq. [32] and [33] will generate two straight lines, and the slopes and intercepts will give the forward and backward intrinsic rate constants (k_1^{int}, k_{-1}^{int}, k_2^{int} and k_{-2}^{int}), respectively, for the two steps. As shown in Fig. (6) and (7), two linear relationships are obtained from the plots. Thus, intrinsic rate constants and equilibrium constants for the two steps can be calculated from the two linear relationships and these are listed in Table 2. One can see that step 1 has the highest forward rate constant (k_1^{int}), which is about 10 times higher than its backward rate constant (k_{-1}^{int}). Contrastingly , the backward rate constant for step 2 (k_{-2}^{int}) is much higher than the forward rate constant (k_2^{int}).

The rate constants describe the reaction process postulated earlier. First, the MoO_4 anion which has already diffused close to the goethite surface is attracted to the surface because of the protonated and positively charged surface site; an ion-pair complex is thus formed very rapidly. Second, the MoO_4 anion reaches the oxide surface to break the bond between Fe and the hydroxyls, and the H_2O molecule is released to the bulk solution. Over time, a new bond is established between MoO_4 and Fe at the oxide surface. The latter ligand exchange process (step 2) is slow compared to step 1. Accordingly, step 2 in Eq. [25] is the rate-controlling step in the reaction between MoO_4 and goethite.

APPENDIX 1

Pressure-Jump Apparatus with Conductivity Detection

The p-jump method is based on the fact that chemical equilibria display a more or less marked pressure dependence (Bernasconi, 1976). The dependence is given by the well-known thermodynamic relationship

$$\left(\frac{\partial \ln K}{\partial p}\right)_T = -\frac{\Delta V}{RT} \qquad [1.1]$$

where ΔV is the standard molar volume change of the reaction, p is the pressure, R is the gas constant, and T is the absolute temperature. A pressure perturbation results in the shifting of the equilibrium. The return of the system to the original equilibrium is related to the rates of all the elementary reaction steps. The determination of relaxation time may be used to describe the mechanism of a reaction. Analogous to Eq. [1.1], for a small perturbation, one can write,

$$\frac{\Delta K}{K} = -\frac{\Delta V}{RT}\Delta p. \qquad [1.2]$$

Figure 8 shows the p-jump apparatus (DIA-RPC) used in this study. The main components include the autoclave, pressure pump, two cells and a vacuum pump. The pressure is built up by the pump with water as the pressure transmitter. The sample and reference cell are covered with a plastic membrane which effectively transmits the pressure. A piece of brass membrane (thickness = 0.03 mm) is clamped on one wall of the autoclave with the bayonet socket. When the pressure in the autoclave gets high enough (9.595 MPa), the brass membrane bursts and the pressure in the autoclave returns to ambient pressure within 70 μs. After the membrane bursts, the sample suspension having

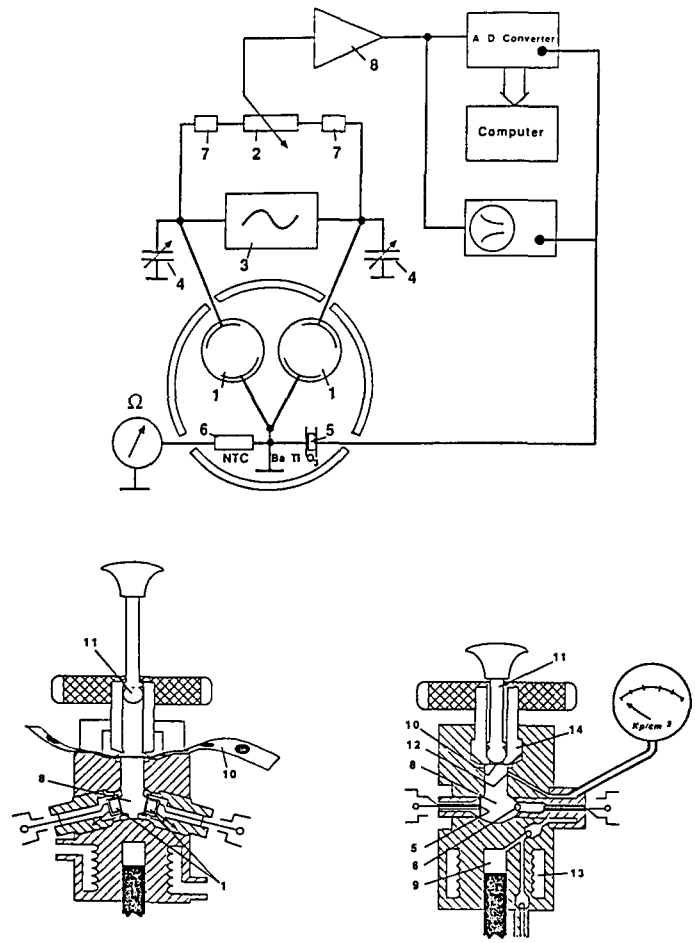

Fig. 8. Schematic diagram and sectional views of the pressure-jump apparatus: (1) conductivity cells; (2) potentiometer; (3) 40-kHz generator for Wheatstone bridge; (4) tunable capacitors; (5) piezoelectric capacitor; (6) thermistor; (7) 10-turn helipot for turning bridge; (8) experimental chamber; (9) pressure pump; (10) rupture diaphragm; (11) vacuum pump; (12) pressure inlet; (13) heat exchanger; (14) bayonet socket. From Knoche and Wiese (1974), with permission.

equilibrium at a higher pressure is out of equilibrium due to the 'instantaneous' pressure jump. The time required to approach equilibrium at the ambient pressure is then monitored by conductivity detection. The cell filled with the non-relaxed background electrolyte ($NaNO_3$) solution is used as a reference which removes the effect of physics such as mechanical and temperature disturbances. Water was circulated in the autoclave to maintain a constant temperature at 298 ± 0.1 K.

Since the equilibrium displacement following a p-jump is usually quite small, the very sensitive conductometric detection method was used in this study (Fig. 8). The specific conductivity, σ (in S m^{-1}), of an electrolyte solution is given by

$$\sigma = \frac{F}{1000}\sum C_j|z_j|\mu_j = \frac{F}{1000}\rho\sum m_j|z_j|\mu_j \qquad [1.3]$$

where F is the Faraday constant, z_j the valence of ion j, C_j the molar and m_j the molality concentrations of ion j, μ_j is the electrical mobility, and ρ is the density of the solution. One can write an equation for a small perturbation as

$$\Delta\sigma = \frac{F}{1000}\left(\rho\sum|z_j|\mu_j\Delta m_j + \rho\sum|z_j|m_j\Delta\mu_j + \sum|z_j|m_j\mu_j\Delta\rho\right). \qquad [1.4]$$

The first term on the right hand side of Eq. [1.4] corresponds to chemical relaxation. The other terms are "physical effects," i.e., the change in ionic mobility and density as a consequence of pressure and temperature changes. However, problems caused by physical effects were eliminated by using a reference cell filled with a nonrelaxed solution ($NaNO_3$) which had the same temperature dependence on conductivity as the sample cell. The change in conductivity in this case corresponds only to the change in concentration of reactants or products. A Wheatstone bridge was set up to measure the change in conductivity in sample and reference cells which are the two arms of the bridge (Fig. 8). The bridge was operated at a frequency of 40 kHz which was greater than the τ^{-1} values that were measured.

APPENDIX 2

For the adsorption-desorption reaction,

$$SOH_2^+ + MoO_4^{2-} \rightleftharpoons SOH_2^+ - MoO_4^{2-} \rightleftharpoons SMoO_4^- + H_2O \quad [2.1]$$

the general forms for relationships between reciprocal relaxation times (τ^{-1}) and other terms associated with the reaction in Eq. [2.1] can be derived as (Bernasconi, 1976)

$$\tau_1^{-1} = 1/2(a_{11} + a_{22}) + \{[1/2(a_{11} + a_{22})]^2 + a_{12}a_{21} - a_{11}a_{22}]^{1/2} \quad [2.2]$$

$$\tau_2^{-1} = 1/2(a_{11} + a_{22}) - \{[1/2(a_{11} + a_{22})]^2 + a_{12}a_{21} - a_{11}a_{22}]^{1/2} \quad [2.3]$$

where

$$a_{11} = k_1([SOH_2^+] + [MoO_4^{2-}]) + k_{-1} \quad [2.4]$$

$$a_{12} = k_{-1} \quad [2.5]$$

$$a_{21} = k_2 \quad [2.6]$$

$$a_{22} = k_2 + k_{-2}. \quad [2.7]$$

In the case when $k_1[(SOH_2^+) + (MoO_4^{2-})] + k_{-1} \gg k_2, k_{-2}$, τ_1^{-1} and τ_2^{-1} are derived as,

$$\tau_1^{-1} = k_1([SOH_2^+] + [MoO_4^{2-}]) + k_{-1} \quad [2.8]$$

$$\tau_2^{-1} = k_2\frac{k_1([SOH_2^+] + [MoO_4^{2-}])}{k_1([SOH_2^+] + [MoO_4^{2-}]) + k_{-1}} + k_{-2} \quad [2.9]$$

Considering the effect of the double electrostatic layer where,

$$K_1^{int} = \frac{[SOH_2^+ - MoO_4^{2-}]}{[SOH_2^+][MoO_4^{2-}]} \exp\left(\frac{F(\psi_\alpha - 2\psi_\beta)}{RT}\right) \quad [2.10]$$

$$K_1^{int} = \frac{k_1^{int}}{k_{-1}^{int}} = K_1 \exp\left[\frac{F(\psi_\alpha - 2\psi_\beta)}{RT}\right] \quad [2.11]$$

$$K_2^{int} = \frac{[SMoO_4^-]}{[SOH_2^+ - MoO_4^{2-}]} \exp\left(\frac{-F\psi_\alpha}{Rt}\right) \quad [2.12]$$

$$K_2^{int} = \frac{k_2^{int}}{k_{-2}^{int}} = K_2 \exp\left(\frac{-F\psi_\alpha}{RT}\right) \quad [2.13]$$

one obtains

$$\tau_1^{-1} = k_1^{int}\left\{\exp\left[\frac{-F(\psi_\alpha - 2\psi_\beta)}{RT}\right]([SOH_2^+] + [MoO_4^{2-}])\right\} + k_{-1}^{int}\exp\left[\frac{F(\psi_\alpha - 2\psi_\beta)}{2RT}\right] \quad [2.14]$$

$$\tau_2^{-1} = k_2^{int}\left[\exp\left(\frac{F\psi_\alpha}{2RT}\right)\left\{k_1^{int}\exp\left[\frac{-F(\psi_\alpha - 2\psi_\beta)}{2RT}\right]([SOH_2^+] + [MoO_4^{2-}])\right\} \Big/ \left\{k_1^{int}\exp\left[-\frac{F(\psi_\alpha - 2\psi_\beta)}{2RT}\right]([SOH_2^+] + [MoO_4^{2-}]) + k_{-1}^{int}\exp\left[\frac{F(\psi_\alpha - 2\psi_\beta)}{2RT}\right]\right\}\right] + k_{-2}^{int}\exp\left(\frac{-F\psi_\alpha}{2RT}\right). \quad [2.15]$$

REFERENCES

Atkinson, R.J., A.M. Posner, and J.P. Quirk. 1967. Adsorption of potential determining ions at the ferric oxide-aqueous electrolyte interface. J. Phys. Chem. 71:550–558.

Bernasconi, C.F. 1976. Relaxation kinetics. Academic Press, New York.

Carter, D.L., M.M. Mortland, and W.D. Kemper. 1986. Specific Surface. *In* A. Klute (ed.) Methods of soil analysis, Part 1. 2nd Edition. Agronomy 9:413–422.

Davis, J.A., and J.O. Leckie. 1980. Surface ionization and complexation at the oxide/water interface. J. Colloid Interface Sci. 74:32–43.

Hachiya, K., M. Ashida, M. Sasaki, H. Kan, T. Inoue, and T. Yasunaga. 1979. Study of kinetics of adsorption-desorption of Pb^{2+} on $\gamma - Al_2O_3$ surface by means of relaxation techniques. J. Phys. Chem. 83:1866–1871.

Hachiya, K., M. Ashida, M. Sasaki, M. Karasuda, and T. Yasunaga. 1980. Study of the adsorption-desorption of IO_3^- on a TiO_2 surface by means of relaxation techniques. J. Phys. Chem. 84:2292–2296.

Hayes, K.F., and J.O. Leckie. 1986. Mechanism of lead ion adsorption at the goethite/water interface. p. 114–141. *In* J.A. Davis and K.F. Hayes (ed.) Geochemical processes at mineral surfaces. ACS Symp. 323. 190th Meet. Am. Chem. Soc., 8–13 Sep. 1985, Chicago. ACS, Washington, DC.

Hayes, K.F., and J.O. Leckie. 1987. Modeling ionic strength effects on cation adsorption at the hydrous oxide/solution interface. J. Colloid Interface Sci. 115:564–572.

Hingston, F.J., A.M. Posner, and J.P. Quirk. 1974. Anion adsorption by goethite and gibbsite. II. Desorption of anions from hydrous oxide surfaces. J. Soil Sci. 25:16–26.

Ikeda, T., M. Sasaki, K. Hachiya, R.D. Astumian, T. Yasunaga, and Z.A. Schelly. 1982. Adsorption-desorption kinetics of acetic acid on silica-alumina particles in aqueous suspensions using the pressure-jump relaxation method. J. Phys. Chem. 86:3861–3866.

Knoche, W., and G. Wiese. 1974. An improved apparatus for pressure-jump relaxation methods. Chem. Instrument 5:91–98.

Mott, C.J.B. 1981. Anion and ligand exchange. p. 179–219. *In* D.J. Greenland and M.H.B. Hayes (ed.) The chemistry of soil processes. John Wiley, New York.

Negishi, H., M. Sasaki, T. Yasunaga, and M. Inoue. 1984. Intercalation kinetics of Na^+ ion into TiS_2 using the pressure-jump technique. J. Phys. Chem. 88:1455–1457.

Parfitt, R.L., 1978. Anion adsorption by soils and soil materials. Adv. Agron. 30:1–50.

Rai, D., and I.P. Murarka. 1987. Evaluation of fundamental data needed to predict the geochemical behavior of elements. p. 101–114. *In* L.L. Boersma et al. (ed.) Future developments in soil science research. SSSA, Madison, WI.

Sparks, D.L. 1987. Kinetics of soil chemical processes: Past progress and future needs. p. 61–74. *In* L.L. Boersma et al. (ed.) Future developments in soil science research. SSSA, Madison, WI.

Sparks, D.L. 1989. Kinetics of soil chemical processes. Academic Press, New York.

Sposito, G. 1985. Chemical models of inorganic pollutants in soils. CRC Crit. Rev. Environ. Control 15:1–24.

Westall, J.C. 1982. FITEQL, A program for determination of chemical equilibrium constants from experimental data (Version 2). Chemistry Dep., Oregon State Univ., Corvallis, OR.

Wedler, G. 1976. Chemisorption, an experimental approach. Trans. by D.F. Klemperer. Butterworth and Co., Boston, MA.

ERRATA

Kinetics and Mechanisms of Molybdate Adsorption/Desorption on the Goethite/Water Interface Using Pressure-Jump Relaxation

PENG CHU ZHANG AND DONALD L. SPARKS

Soil Sci. Soc. Am. J. 53:1028–1034 (July–Aug. 1989).

The exponential term $F(\psi_\alpha - \psi_\beta)/RT$ in Eq. [9], [10], and [12] should read $-F\psi_\beta/RT$. The term $\exp[F(\psi_\alpha - 2\psi_\beta)/RT]$ in Eq. [11] should read $\exp(-2F\psi_\beta/RT)$. The term $\exp(-F\psi_\alpha/RT)$ in Eq. [23] should be $\exp(-2F\psi_\alpha/RT)$. The exponential terms in the equations that were derived from Eq. [11] and [23] should read $\exp[F(\psi_\alpha - 2\psi_\beta)/RT]$ and $\exp(-2F\psi_\beta/RT)$, respectively.